International Journal of Chemistry; Vol. 7, No. 2; 2015
ISSN 1916-9698 E-ISSN 1916-9701
Published by Canadian Center of Science and Education

# Voltammetry of Suspensions of Polyaniline-coated Graphene Composites

Jingyuan Chen[1], Xiangdong Zeng[1], Koichi Jeremiah Aoki[2], Toyohiko Nishiumi[1]

[1]Department of Applied Physics, University of Fukui, Fukui, Japan

[2]Electrochemistry Museum, Fukui, Japan

Correspondence: Jingyuan Chen, Department of Applied Physics, University of Fukui, 3-9-1 Bunkyo, Fukui, 910-0017, Japan. E-mail jchen@u-fukui.ac.jp, Tel: +81 776 27 8753

Received: May 16, 2015 Accepted: June 2, 2015 Online Published: July 6, 2015

doi:10.5539/ijc.v7n2p1 URL: http://dx.doi.org/10.5539/ijc.v7n2p1

**Abstract**

Flaky particles of polyaniline (PANI)-graphene (GN) with rectangular size of 1.0-1.5 μm are dispersed in aqueous solution so that their suspension is stable for one day without aggregation. The weight fraction of PANI in the particle is 75 %, which is independent of the loaded fraction of PANI in the synthesis. The PANI-GN film made of the suspension forms a self-standing, elastic, conductive film. The PANI-GN suspension exhibits both the reduction and the oxidation waves at potentials similar to those of PANI adsorbed on an electrode, whereas the PANI-GO suspension shows only the voltammetric reduction wave. The redox peak currents are controlled by diffusion of PANI-GN flakes. The PANI-GN film cast on the electrode shows voltammetric peaks for PANI, of which redox charge is larger than that of the electrochemically polymerized PANI film with the common weight of PANI. This fact can be explained in terms of the electrochemically exhaustive oxidation of PANI through the electric conduction of GN.

**Keywords**: polyaniline-coated grapheme, self-standing film of polyaniline, voltammetry in dispersed particles, diffusion-controlled current of flaky particles

## 1. Introduction

Graphene (GN) is a promising material of super capacitors because its two-dimensional $sp^2$-hybridized carbon sheet provides extremely large surface area in contact with solution (Segal, 2009; Feng et al., 2011). GN sheets have been generated through the processes by the oxidation of graphite in the form of suspensions (Staudenmaier, 1898; Schniepp, et al., 2006; Stankovich, et al., 2006; Dreyer, et al., 2010; Pan & Aksay, 2011; Singh et al., 2011), called the Hummers method (Hummers & Offeman, 1958), and then by the chemical reduction of the suspensions to GN. Once GN flakes are formed, they are aggregated gradually to the original graphite form (Yang et al., 2011; Yi et al., 2014).

Suspensions of GN and/or graphite oxide (GO) flakes have been stabilized with organic solvents (Park et al., 2009; Zhang & Zhao, 2012), organic salt (Zhang et al., 2014) and conducting polymers (Higashika et al., 1999; Xiao et al., 2000; Bourdo & Viswanathan, 2005; Lu et al., 2011; Luo et al., 2013) against agglomeration. The stabilized GN films have been used for enhancing photocurrents (Chatterjee et al., 2013), electrocatalytic activity (Yang et al., 2014), the charge density of supercapacitors (Wang et al., 2009; Yan et al., 2010; Chen et al., 2012; Sarker & Hong, 2012; Zhang & Zhao, 2012; Gao et al., 2013; Giri et al., 2013; Luo et al., 2013; Sawangphruk et al., 2013; Zhang et al., 2013; Gao et al., 2014; Heli & Yadegari, 2014; Xiong et al., 2014; Yu et al., 2014) and performance of dye-sensitized solar cells (Wang et al., 2012). Supercapacitors, made of conducting polymer and GN composite, which can provide huge charge density (Zhang et al., 2013), may be one of the most successful applications of GN. The high charge density results from both the double layer capacity and the redox reaction of conducting polymers, especially polyaniline (PANI). The roles of PANI of the PANI-GN composite are i) to keep electric connection of GN flakes with PANI so that all the flakes on the electrode are electrically percolated (Yan et al., 2010; Gao et al., 2013; Zhang et al., 2013), and ii) to utilize charge of the redox reactions of PANI (Luo et al., 2013; Xiong et al., 2014). Although the two roles are different in the mechanisms, it is difficult to evaluate each contribution quantitatively. Especially, the redox charge of the adsorbed PANI cannot be readily distinguished from the capacitive charge of PANI and that of GN.

If the observed charge of PANI-GN composites is a simple sum of the redox charge of PANI and the capacitive charge of GN and PANI in accord with the weight ratio of PANI and GN, the advantages of the composites would be so worthless as to be explored. Much attention to the PANI-GN composites suggests participation in synergetic effects of PANI and GN. In order to find the synergetic effects, it is necessary to find relationships between the weight ratio and the charge ratio, and between properties of the composites and those of individual species. We are concerned with finding these relations in this report by use of PANI-GN suspension, because suspensions can be prepared generally by controlling interactions among dispersed particles.

## 2. Experimental

Water was distilled and then ion-exchanged by an ultrapure water system, CPW-100 (Advantec, Tokyo). All the chemicals were of analytical grade. Graphite powder (98%, 7 μm in average diameter) was purchased from Ito Koken (Mie, Japan), and was used as it was.

Graphite oxide (GO) was generated basically according to the reported processes (Hummers & Offeman, 1958). The Crude product was centrifuged with a cooling centrifugal machine (Tomy, Tokyo) at the maximum 10600 *g* for 5 min. The supernatant by the centrifugation was dispersed in pure water, and then was centrifuged at 4 $^{o}$C, 7000 *g* to purify. This process was iterated three times. An aliquot of the refined GO suspension was dried and weighed to determine the weight concentration. A given amount of the GO suspension was added to a given amount of the solution of 0.15 M (= mol dm$^{-3}$) aniline hydrochloride + 0.5 M sulfuric acid. The oxidant, ammonium peroxydisulfate, with 1.3 times amount of aniline was added to the mixture, and was kept for 1 day in an ice bath. The suspension was dispersed to 0.5 M sulfuric acid and was centrifuged. The sediment was dried under vacuum at 40$^{o}$C for 6 h.

In order to reduce the PANI-GO composite, 0.1 cm$^3$ hydrazine monohydrate was added to 50 cm$^3$ suspension including 0.1 g dried PANI-GO. The mixture was put in a bath at 95$^{o}$C for 1 h. The product was dispersed in 0.5 M sulfuric acid, and centrifuged. The dispersion-centrifugation process was iterated until the supernatant showed no absorbance band of PANI in the visible wave length domain. The iteration was normally three or four times. The sediment was dispersed in 1% of polyvinylpyrrolidone + 0.5 M sulfuric acid. The dispersion was centrifuged at 6000 *g* to be separated into three vague layers. The middle part was used for the samples of the reduced PANI-GN composite.

Cyclic voltammetry was carried out with a potentiostat, Compactstat (Ivium Tech., Netherlands). The reference electrode was Ag|AgCl in saturated KCl. The counter electrode was a platinum wire. The working electrode was the platinum disk 1.6 mm in diameter.

The size distribution of latex particles was determined by a dynamic light scattering (DLS) instrument (Malvern Zetasizer Nano-ZS, UK). Thermogravimetric analyses (TGA) was carried out with Thermo Plus, TG8120 (Rigaku, Tokyo), on which the amount of the sample, ca. 5.0 mg, was mounted. Temperature was increased at 10$^{o}$C min$^{-1}$ under nitrogen atmosphere. SEM photographs were taken with JSM-6701F (JEOL, Tokyo).

## 3. Results and Discussion

### *3.1 Compositions of Polyaniline-composites*

The PANI-GO-composite suspension, being green, had no sedimentation for 1 day, as the GO is well suspended. The PANI-GO suspension, which was reduced with hydrazine, got dark green and had also no sedimentation. Since GO may be reduced to GN, we call it PANI-GN. On the other hand, the reduced GO without PANI was agglomerated soon. Therefore PANI works as a surfactant of dispersing GO or GN. Fig. 1 shows photograph of the PANI-GN composite suspension (in the wet state) by an optical microscope. Some angulate particles are found, which may be GN flakes coated with PANI. Those in the suspension were oscillating by the Brownian motion, as shown in the movie of Supplement. The Brownian motion indicates the capability of transport of the particle by diffusion. We paid attention to a moving particle in a frame of the movie, and read the lengths of the particle along the *x*- and *y*-directions at each 0.1 s. The lengths are plotted against the time in Fig. 1 (insert). The time-variations indicate the Brownian motion of the flake particle, changing the orientation of the flake. The maximum and the minimum lengths may be close to the projected ones of the flake, depending on directions. The PANI-GO suspension had almost the same optical microscopic view as in Fig. 1.

A given volume of the PANI-GN suspension was dried on a carbon tape. Fig. 2(A) shows a SEM image of the dried suspension. Rectangular flakes appear, in comparison with the PANI film (B). The images of the PANI-GN were always clearer than those of the PANI, probably because of its higher conductivity than PANI.

Fig. 3 shows the size-distribution of the PANI-GN, where the size represents a diameter at which a rectangular particle is approximated as a circle in the photograph of Fig. 1. The diameters range from 1 μm to 1.5 μm, which

is close to the length of rectangular flakes in Fig. 2(A). The supernatant of the centrifuged suspension was transparent. Since it did not show any redox wave by cyclic voltammetry in the potential domain from -0.1 V to 0.8 V vs Ag|AgCl, it contains no oligo-aniline or dissolved PANI. Consequently, PANI is immobilized on the suspended GN particles.

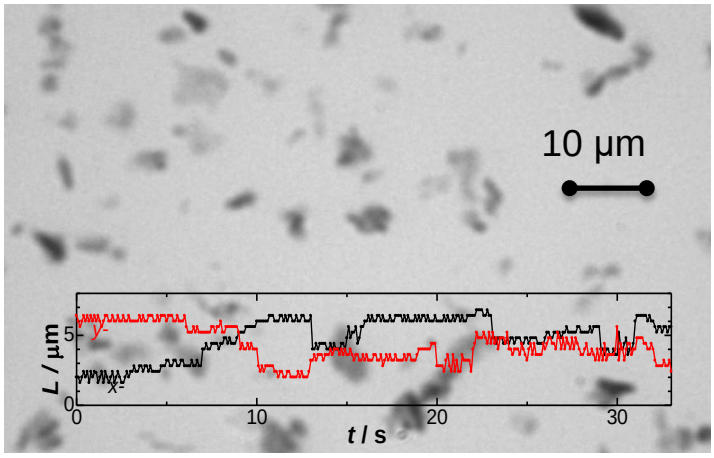


Fig. 1. Photograph of the wet PANI-GO suspension by the optical microscope, and (insert) the plot of lengths, *L*, of a particle along *x*- and y-directions against the time by the randomly rotational motion.

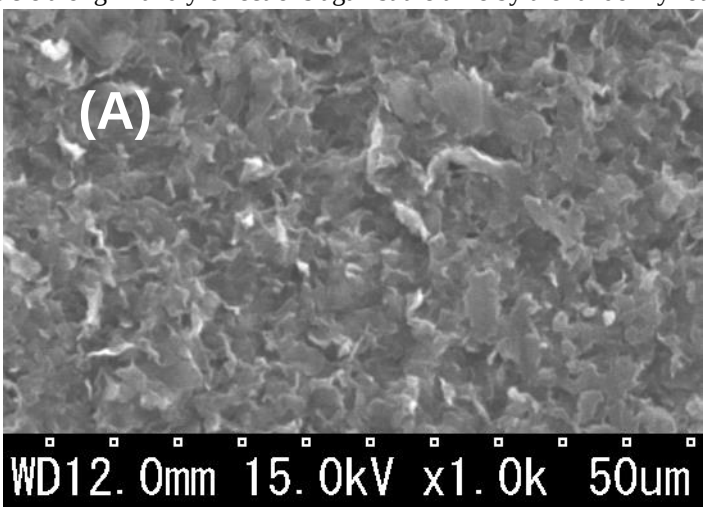


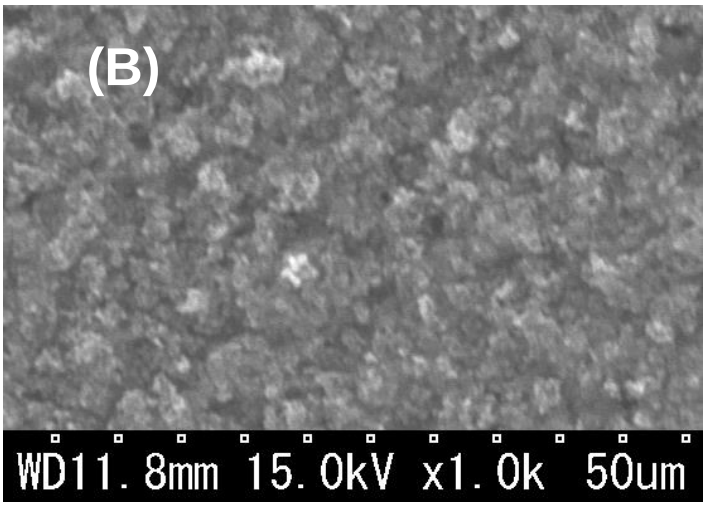


Fig. 2. SEM of (A) PANI-GN, and (B) PANI.

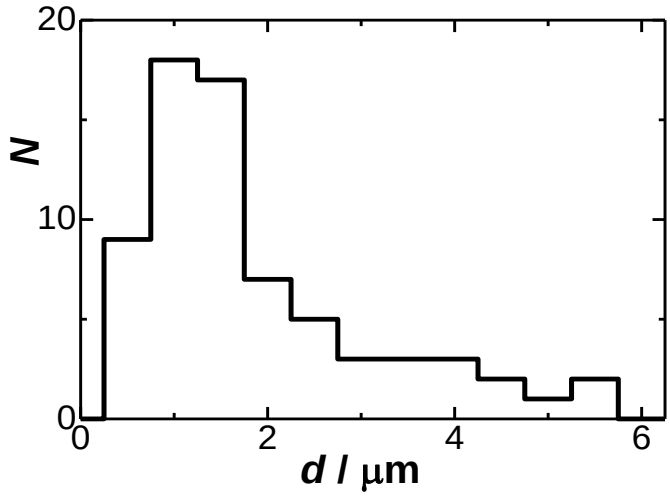


Fig. 3. Distribution of size of suspended PANI-GN particles synthesized at weight fraction of aniline to graphite was 3:1.

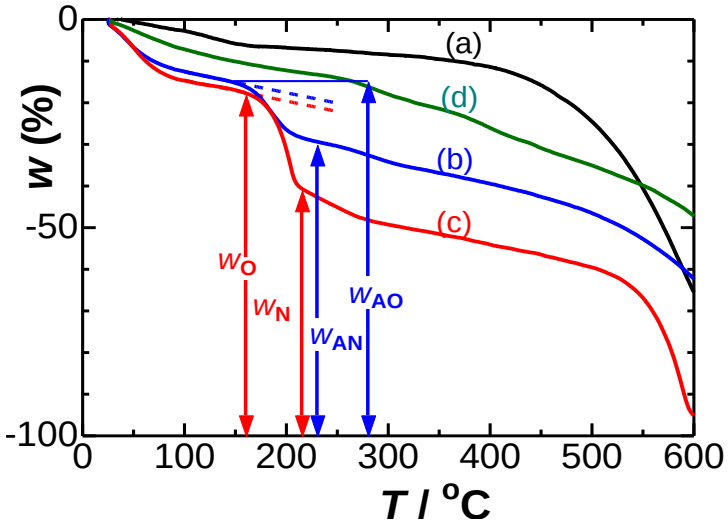


Fig. 4. Thermogravimetric curves of (a) PANI, (b) PANI-GO, (c) GO and (d) reduced PANI-GO, obtained at the rate of the rising temperature, 10 $^{o}$C min$^{-1}$.

In order to obtain the weight ratio of PANI to the PANI-GN or PANI-GO particles, we carried out thermogravimetriry. Fig. 4 shows thermogravimetric curves of (a) PANI, (b) PANI-GO, (c) GO and (d) PANI-GN. The decrease in the weight at temperature lower than 140 $^{o}$C is ascribed to evaporation of water. The chemical structure of PANI was kept almost constant until 400 $^{o}$C (curve (a)). GN is reportedly decomposed at temperature over 500 $^{o}$C into CO and $CO_2$ to be volatilized (Lerf et al., 1998; Choi et al., 2010). This weight loss to zero was seen not only for PANI-GN (d) but also for PANI-GO (b) and GO (c). The loss of GO in the domain 170-200 $^{o}$C (c) is found in all the GO-included particles. Therefore it can be ascribed to the decomposition of GO into GN. The weights at 170 $^{o}$C and 220 $^{o}$C in the TGA curve for GO (c) represent weights of GO and GN, respectively, denoted by $w_O$ and $w_N$. In contrast, the weights for PANI-GO (b) at 170 $^{o}$C and 220 $^{o}$C represent those of PANI+GO and PANI+GN, respectively, denoted by $w_{AO}$ and $w_{AN}$. From these values we determined some ratios, subtracting the backgrounds (dashed lines in Fig. 4); $w_N/w_O = 0.74$, $w_{PANI}/w_O = 1.13$ and $w_{PANI}/w_N = 1.53$. As a result, the weight amount of PANI is of the same order of magnitude of that of GN.

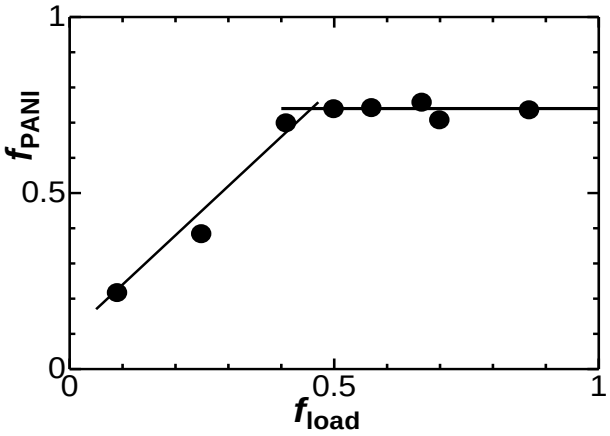


Fig. 5. Variations of the fraction of PANI in the PANI-GO with the fraction of loaded PANI at the synthesis.

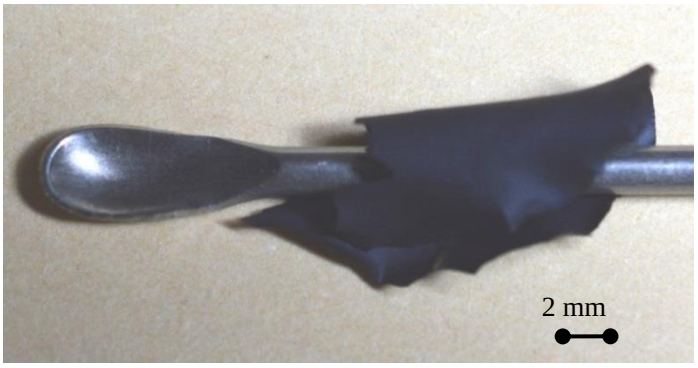


Fig. 6. Photographs of self-standing films of PANI-GN, which was curled in a spatula.

We varied the loaded concentration of aniline in the synthesis so that the fraction of loaded weight concentration of aniline ranged from 0.09 to 0.87. The weight fraction of PANI to PANI-GO is given by $f_{PANI} = w_{PANI} / (w_{PANI} + w_O)$, determined with TGA. Fig. 5 shows plot of $f_{PANI}$ against the fraction of the loaded aniline at the synthesis, $f_{load}$ ( $= w_{aniline}/(w_{aniline} + w_{loaded\ O})$). The value of $f_{PANI}$ increased linearly with $f_{load}$ for $f_{load} < 0.4$, and reached a saturated value, $0.73 \pm 0.02$. The saturated values for PANI-GN, i.e. $w_{PANI}/(w_{PANI} + w_N)$, is calculated to be $0.79 \pm 0.02$. The linear domain indicates that the amount of aniline ran short of the polymerization to produce partially PANI-covered GO flakes. The saturation implies that GO flakes should be coated with a given thickness of PANI films without further growth on the PANI film, similar to the films by the surface-initiated polymerization (Zhu et al., 2012).

As a drop of the suspension of PANI-GN was dried on a substrate such a glass plate, a metal surface and a sheet of paper, it was gradually peeled off from the substrate in a rolled form to generate a self-standing film. It was able to be readily carried with a pair of tweezers or a spatula or, as shown in Fig. 6. The PANI-GN film was as big as 1 $cm^2$ squares in rolled form, of which thickness was ca. 34 μm. It was electrically conducting, and the resistance was 8 kΩ between two needle-like terminal pins of a resistance meter with 5 mm separation. The film was so elastic that the rolled shape was not deformed after the resistance measurement by pressing the film with the two pins. It was not destroyed when it was dropped from 1 m height. The PANI-GO suspensions also generate self-standing films. However, the size was smaller than that of PANI-GN films because of fragility. PANI films are too brittle to generate self-standing films.

*3.2 Voltammetry*

Mass transport properties of suspensions are revealed in the voltammetric behavior (Chen, & Zhang, 2005; Aoki & Ke, 2006; Chen, et al., 2006; Han, et al., 2007; Chen, et al., 2008). Voltammograms in the PANI-GN suspension at the naked platinum electrode are shown in Fig. 7(a)-(c) for some scan rates, where the potential scan was started at the open circuit potential, 0.1 V. They did not vary with the number of scans. There was no adsorbed particle on the electrode surface after voltammetry from the view of the optical microscope. The voltammograms have both the reduction wave and the oxidation wave at potentials close to those of the

electrochemically polymerized PANI (Fig. 7(d)). Therefore PANI in the PANI-GN suspension is both reduced and oxidized reversibly. This reversibility is a contrast to the voltammograms of the PANI-GO suspension (in Fig. 8), in which no anodic wave appears. Since the PANI-GO cast film exhibited the voltammograms similar to at the PANI-coated electrode (Fig. 7(d)), the disappearance of the anodic wave in the suspension (Fig. 8) should be ascribed to the dispersion of particles. The waves similar to Fig. 8 have been observed at polystyrene-coated PANI latex suspensions (Chen et al., 2008), in which the disappearance of the anodic wave has been attributed to the suppression of the oxidation by the propagation of the conducting zone of PANI (Aoki et al., 1992; Aoki et al., 1993; Aoki & Kawase, 1994; Cao & Aoki, 1996). In general, dispersed particles of the reduced PANI may not be oxidized electrochemically because they are detached from the electrode before completing the oxidation over the whole particle (Chen et al., 2006).

The anodic and the cathodic peak currents in Fig. 7 were approximately proportional to $v^{1/2}$, as are shown in Fig. 8(e) and (e'). The proportionality indicates that the currents should be controlled by diffusion of the PANI-GN particles. According to the derivation of the diffusion-controlled voltammetric current for the *n*-sequential electron transfer reaction of the redox species (Aoki, 2005), the peak current is expressed by

$$I_p = \pm 0.446\, nec^* A(DvF/RT)^{1/2} \quad (1)$$

where $D$ is the diffusion coefficient of the redox particle, $A$ is the area of the electrode, $c^*$ is the number concentration of the particle, and $n$ is the number of electrons relevant to the electrode reaction per particle. The difference of Eq. (1) from the Randles-Sevich equation is the first order of $n$ rather than $n^{3/2}$. We determined the charge concentration of PANI-GN suspension, $nec^*$, from the charge per mass of the dried suspension and the weight concentration of the suspension. The slope in inset Fig. 8 should be equal to $\pm 0.446\, nec^* A(DF/RT)^{1/2}$. From the known values of $nec^*$ and $A$, we evaluated $D$ to be $2.9\times10^{-9}$ cm$^2$ s$^{-1}$. When the Stokes-Einstein equation is applied to the $D$-value by use of the viscosity of water at 25°C, the diameter of the PANI-GN particles is 1.6 μm. This value is similar to the values obtained by the optical microscope (in Fig. 1).

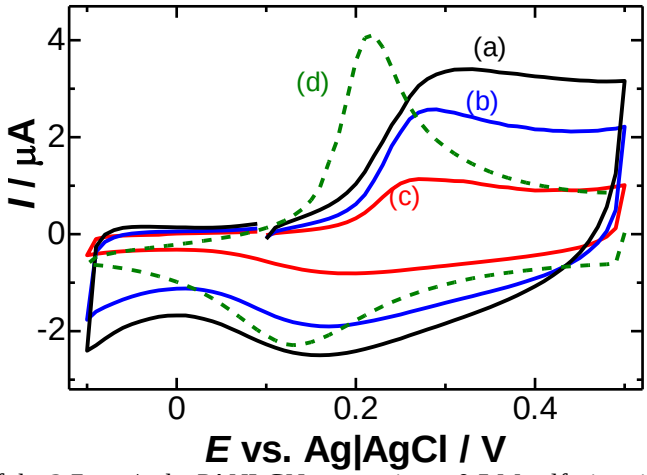


Fig. 7. Voltammograms of the 2.7 mg /g the PANI-GN suspension + 0.5 M sulfuric acid at the platinum electrode for $v$ = (a) 100, (b) 50 and (c) 10 mV s$^{-1}$. Voltammogram (d) is at the electrochemically polymerized PANI electrode in 0.5 M sulfuric acid for $v$ = 10 mV s$^{-1}$.

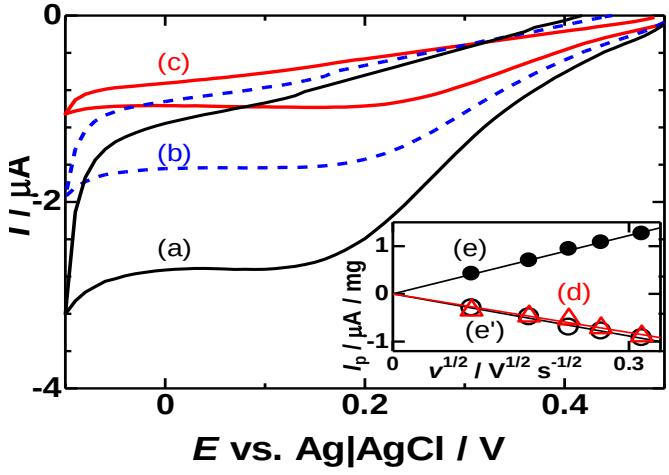

Fig. 8. Voltammograms of the 2.6 mg /g the PANI-GO suspension + 0.5 M sulfuric acid at the platinum electrode for $v$ = (a) 100, (b) 50 and (c) 10 mV $s^{-1}$. The inset shows variations of the peak currents with the square roots of the scan rates for (d) the PANI-GO suspension and (e) the PANI-GN suspension.

In order to evaluate the redox charge of PANI in the PANI-GN suspension, we cast a given amount of the suspension on the platinum electrode and dried it under vacuum at 40 $^{o}$C for 6 h. The dried film did not disperse in the aqueous solution. Figure 9 shows the voltammograms of the film (a) in 0.5 M sulfuric acid, together with the film made of the PNANI-GO suspension (b) and the electropolymerized PANI film (c), where the current values were normalized with 1.0 μg PANI. The voltammogram of PANI-GO is almost the same as that of the PANI film, indicating that GO does not contribute to the current without any effect on the redox reaction of PANI. In contrast, the voltammogram of PANI-GN (a) is three times larger than that of PANI-GO (b). The larger current may be ascribed to the electric conduction of GN. When the PANI-GO film was reduced on the electrode with hydrazine for 1 h, the voltammetric current (d) was smaller than that of the PANI-GN film. The smaller voltammogram indicates that the reduction of GO to GN in the film should be not be completed. This is advantage of the process of fabricating of the PANI-GN films by use of the PANI-GN suspensions.

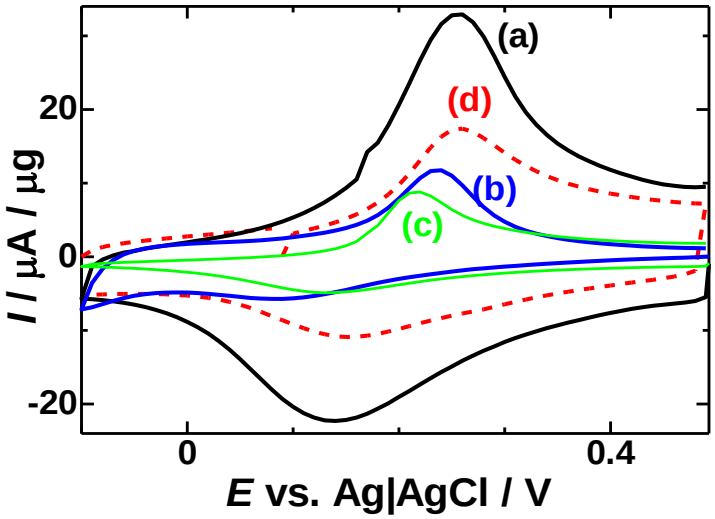


Fig. 9. Voltammograms of the films which were formed by casting and drying (a) PANI-GN, (b) PANI-GO, (c) the electropolymerized PANI film, and (d) the PANI-GO film (b) reduced with hydrazine. They were obtained in 0.5 M sulfuric acid at the platinum electrode for $v$ = 10 mV $s^{-1}$. The current values were normalized with 1.0 μg PANI.

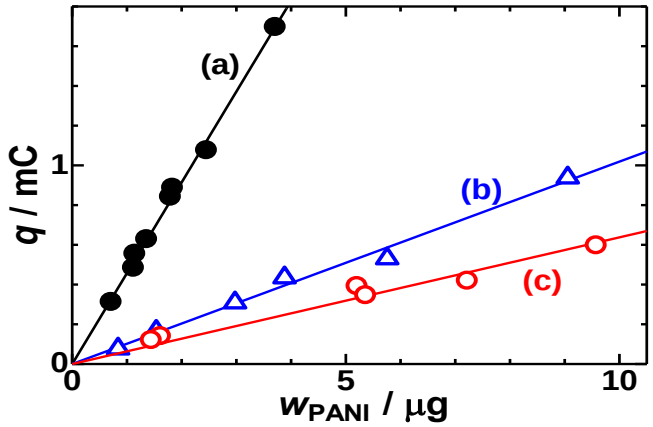


Fig. 10. Dependence of the oxidation charge of PANI for the (a) PANI-GN, (b) PANI-GO and (c) PANI films on the amount of PANI loaded on the electrode.

We evaluated the oxidation charge from the peaked part, and plotted the charge against thickness of the films in Fig. 10. Since the peak is caused by the redox reaction of PANI, the area of the peak should stand mostly for the amount of the redox charge of PANI rather than the capacitive charge of GN. The latter should appear as a

background-like current without peak. The charges of the three kinds of films are proportional to the thickness. Therefore the local redox reaction occurring at a position far from the electrode ought to have no effect of electric resistance. The slope for the PANI-GN is 4.5 times larger than that of PANI-GO although the amount of PANI loaded on the electrode is common. We can explain the difference in terms of the incompleteness of the electrochemical reduction of PANI (Aoki et al., 1993; Aoki & Kawase, 1994; Cao & Aoki, 1996) in which some parts of oxidized PANI is left behind from the electrochemical reduction because of cut-off of the electric percolation during the reduction. The use of PANI-GN suspensions overcomes the difficulty in incomplete redox reaction of PANI films. The slope for the PANI-GO is slightly larger than that of PANI. This is probably because the GO flakes expose conducting carbon surface locally with which PANI makes an electric contact.

## 4. Conclusions

Not only PANI-GO but also PANI-GN particles are dispersed in acidic solutions, exhibiting the Brownian motion. A side length of a rectangular PANI-GN flake ranges from 1 to 1.5 μm. The weight fraction of PANI to PANI-GN is a constant, 0.79, regardless of the loaded fractions larger than 0.4. The constant value indicates that GO flakes should be coated with a given thickness of PANI films without further growth on the PANI film. The PANI-GN suspension generates a self-standing large film, which is elastic and electrically conductive. In contrast, the film made of the PANI suspension is fragile and has small size.

The PANI-GN suspension shows both the reduction and the oxidation waves, whereas the PANI-GO suspension exhibits only the reduction wave. The electric conduction of GN can oxidize electrochemically the reduced (insulating) PANI without the slow process of the propagation of the conducting zone. The voltammetric peak current of the PANI-GN suspension is controlled by diffusion of the PANI-GN flakes. The cast film of the PANI-GN suspension on the electrode shows the voltammetric currents 4.5 times larger than the films of PANI-GO. This can be understood by the electric conduction of GN, which compensates the electrochemical irreversibility of the redox charge of PANI.

## Acknowledgment

This work was financially supported by Grants-in-Aid for Scientific Research (Grant 25420920) from the Ministry of Education in Japan.

## References

Aoki, K. (2005). Is Voltammetric Current Proportional to the Number of Transferred Electrons for Multi-Charged Ions or to 3/2 Power of the Number? *Electroanalysis*, *17*(15-16), 1379-1383. http://dx.doi.org/10.1002/elan.200403285

Aoki, K., & Kawase, M. (1994). Introduction of a Percolation-Threshold Potential at Polyaniline-Coated Electrodes. *Journal of Electroanalytical Chemistry*, *377*(1-2), 125-129. http://dx.doi.org/10.1016/0022-0728(94)03446-X

Aoki, K., & Ke, Q. (2006). Voltammetric discrete current of polyaniline-coated latex particles at microelectrodes. *Journal of Electroanalytical Chemistry*, *587*(1), 86-92. http://dx.doi.org/10.1016/j.jelechem.2005.10.019

Aoki, K., Aramoto, T., & Hoshino, Y. (1992). Photographic measurements of propagation speeds of the conducting zone in polyaniline films during electrochemical switching. *Journal of Electroanalytical Chemistry*, *340*(1–2), 127-135. http://dx.doi.org/10.1016/0022-0728(92)80293-D

Aoki, K., Cao, J. A., & Hoshino, Y. (1993). Coulombic Irreversibility at Polyaniline-Coated Electrodes by Electrochemical Switching. *Electrochimica Acta*, *38*(13), 1711-1716. http://dx.doi.org/10.1016/0013-4686(93)85066-8

Bourdo, S. E., & Viswanathan, T. (2005). Graphite/Polyaniline (GP) composites: Synthesis and characterization. *Carbon*, *43*(14), 2983-2988. http://dx.doi.org/10.1016/j.carbon.2005.06.016

Cao, J., & Aoki, K. (1996). Percolation threshold potentials at quasi-static electrochemical switching of polyaniline films. *Electrochimica Acta*, *41*(11-12), 1787-1792. http://dx.doi.org/10.1016/0013-4686(95)00496-3

Chatterjee, S., Layek, R. K., & Nandi, A. K. (2013). Changing the morphology of polyaniline from a nanotube to a flat rectangular nanopipe by polymerizing in the presence of amino-functionalized reduced graphene oxide and its resulting increase in photocurrent. *Carbon*, *52*, 509-519. http://dx.doi.org/10.1016/j.carbon.2012.10.003

Chen, F., Liu, P., & Zhao, Q. Q. (2012). Well-defined graphene/polyaniline flake composites for high performance supercapacitors. *Electrochimica Acta*, *76*, 62-68. http://dx.doi.org/10.1016/j.electacta.2012.04.154

Chen, H., Chen, J., Aoki, K., & Nishiumi, T. (2008). Electrochemically instantaneous reduction of conducting polyaniline-coated latex particles dispersed in acidic solution. *Electrochimica Acta*, *53*(24), 7100-7106. http://dx.doi.org/10.1016/j.electacta.2008.04.084

Chen, J., & Zhang, Z. (2005). Diffusion-controlled currents of redox latex particles with polystyrene-core and polyallylamine-ferrocenyl shell. *J. Electroanal. Chem.*, *583*, 116-123. http://dx.doi.org/10.1016/j.jelechem.2005.05.008

Chen, J., Aoki, K., Nishiumi, T., & Li, T. B. (2006). Voltammetry of suspensions of hollow particles with ferrocene-immobilized polyallylamine shells. *Langmuir*, *22*(25), 10510-10514. http://dx.doi.org/10.1021/la0610304

Choi, E. Y., Han, T. H., Hong, J. H., Kim, J. E., Lee, S. H., Kim, H. W., & Kim, S. O. (2010). Noncovalent functionalization of graphene with end-functional polymers. *Journal of Materials Chemistry*, *20*(10), 1907-1912. http://dx.doi.org/10.1039/B919074k

Dreyer, D. R., Park, S., Bielawski, C. W., & Ruoff, R. S. (2010). The chemistry of graphene oxide. *Chem Soc Rev*, *39*(1), 228-240. http://dx.doi.org/10.1039/b917103g

Feng, X.-M., Li, R.-M., Ma, Y.-W., Chen, R.-F., Shi, N.-E., Fan, Q.-L., & Huang, W. (2011). One-Step Electrochemical Synthesis of Graphene/Polyaniline Composite Film and Its Applications. *Advanced Functional Materials*, *21*(15), 2989-2996. http://dx.doi.org/10.1002/adfm.201100038

Gao, Z. Y., Wang, F., Chang, J. L., Wu, D. P., Wang, X. R., Wang, X., Xu, F., Gao, S. Y., & Jiang, K. (2014). Chemically grafted graphene-polyaniline composite for application in supercapacitor. *Electrochimica Acta*, *133*, 325-334. http://dx.doi.org/10.1016/j.electacta.2014.04.033

Gao, Z., Yang, W. L., Wang, J., Yan, H. J., Yao, Y., Ma, J., Wang, B., Zhang, M. L., & Liu, L. H. (2013). Electrochemical synthesis of layer-by-layer reduced graphene oxide sheets/polyaniline nanofibers composite and its electrochemical performance. *Electrochimica Acta*, *91*, 185-194. http://dx.doi.org/10.1016/j.electacta.2012.12.119

Giri, S., Ghosh, D., & Das, C. K. (2013). In situ synthesis of cobalt doped polyaniline modified graphene composites for high performance. supercapacitor electrode materials. *Journal of Electroanalytical Chemistry*, *697*, 32-45. http://dx.doi.org/10.1016/j.jelechem.2013.01.038

Han, L. M., Chen, J., & Aoki, K. (2007). Size-dependent efficiency of electron transfer at suspended ferrocenyl jumbo particles. *Journal of Electroanalytical Chemistry*, *602*(1), 123-130. http://dx.doi.org/10.1016/j.jelechem.2006.12.009

Heli, H., & Yadegari, H. (2014). Poly(ortho-aminophenol)/graphene nanocomposite as an efficient supercapacitor electrode. *Journal of Electroanalytical Chemistry*, *713*, 103-111. http://dx.doi.org/10.1016/j.jelechem.2013.12.010

Higashika, S., Kimura, K., Matsuo, Y., & Sugie, Y. (1999). Synthesis of polyaniline-intercalated graphite oxide. *Carbon*, *37*(2), 354-356. http://dx.doi.org/10.1016/S0008-6223(99)90002-7

Hummers, W. S., & Offeman, R. E. (1958). Preparation of Graphitic Oxide. *Journal of the American Chemical Society*, *80*(6), 1339-1339. http://dx.doi.org/10.1021/ja01539a017

Lerf, A., He, H. Y., Forster, M., & Klinowski, J. (1998). Structure of graphite oxide revisited. *Journal of Physical Chemistry B*, *102*(23), 4477-4482. http://dx.doi.org/10.1021/Jp9731821

Lu, X. J., Dou, H., Yang, S. D., Hao, L., Zhang, L. J., Shen, L. F., Zhang, F., & Zhang, X. G. (2011). Fabrication and electrochemical capacitance of hierarchical graphene/polyaniline/carbon nanotube ternary composite film. *Electrochimica Acta*, *56*(25), 9224-9232. http://dx.doi.org/10.1016/j.electacta.2011.07.142

Luo, J., Jiang, S. S., Liu, R., Zhang, Y. J., & Liu, X. Y. (2013). Synthesis of water dispersible polyaniline/poly(styrenesulfonic acid) modified graphene composite and its electrochemical properties. *Electrochimica Acta*, *96*, 103-109. http://dx.doi.org/10.1016/j.electacta.2013.02.072

Luo, Z. H., Zhu, L. H., Zhang, H. Y., & Tang, H. Q. (2013). Polyaniline uniformly coated on graphene oxide sheets as supercapacitor material with improved capacitive properties. *Materials Chemistry and Physics*, *139*(2-3), 572-579. http://dx.doi.org/10.1016/j.matchemphys.2013.01.059

Pan, S., & Aksay, I. A. (2011). Factors controlling the size of graphene oxide sheets produced via the graphite oxide route. *ACS Nano*, *5*(5), 4073-4083. http://dx.doi.org/10.1021/nn200666r

Park, S., An, J., Jung, I., Piner, R. D., An, S. J., Li, X., Velamakanni, A., & Ruoff, R. S. (2009). Colloidal suspensions of highly reduced graphene oxide in a wide variety of organic solvents. *Nano Lett*, *9*(4), 1593-1597. http://dx.doi.org/10.1021/nl803798y

Sarker, A. K., & Hong, J.-D. (2012). Layer-by-Layer Self-Assembled Multilayer Films Composed of Graphene/Polyaniline Bilayers: High-Energy Electrode Materials for Supercapacitors. *Langmuir*, *28*(34), 12637-12646. http://dx.doi.org/10.1021/la3021589

Sawangphruk, M., Suksomboon, M., Kongsupornsak, K., Khuntilo, J., Srimuk, P., Sanguansak, Y., Klunbud, P., Suktha, P., & Chiochan, P. (2013). High-performance supercapacitors based on silver nanoparticle-polyaniline-graphene nanocomposites coated on flexible carbon fiber paper. *Journal of Materials Chemistry A*, *1*(34), 9630-9636. http://dx.doi.org/10.1039/C3TA12194A

Schniepp, H. C., Li, J. L., McAllister, M. J., Sai, H., Herrera-Alonso, M., Adamson, D. H., Prud'homme, R. K., Car, R., Saville, D. A., & Aksay, I. A. (2006). Functionalized single graphene sheets derived from splitting graphite oxide. *J Phys Chem B*, *110*(17), 8535-8539. http://dx.doi.org/10.1021/jp060936f

Segal, M. (2009). Selling graphene by the ton. *Nature Nanotechnology*, *4*(10), 612-614. http://dx.doi.org/10.1038/nnano.2009.279

Singh, V., Joung, D., Zhai, L., Das, S., Khondaker, S. I., & Seal, S. (2011). Graphene based materials: Past, present and future. *Progress in Materials Science*, *56*(8), 1178-1271. http://dx.doi.org/10.1016/j.pmatsci.2011.03.003

Stankovich, S., Dikin, D. A., Dommett, G. H. B., Kohlhaas, K. M., Zimney, E. J., Stach, E. A., Piner, R. D., Nguyen, S. T., & Ruoff, R. S. (2006). Graphene-based composite materials. *Nature*, *442*(7100), 282-286. http://dx.doi.org/10.1038/nature04969

Staudenmaier, L. (1898). Verfahren zur Darstellung der Graphitsäure. *Berichte der deutschen chemischen Gesellschaft*, *31*(2), 1481-1487. http://dx.doi.org/10.1002/cber.18980310237

Wang, G. Q., Xing, W., & Zhuo, S. P. (2012). The production of polyaniline/graphene hybrids for use as a counter electrode in dye-sensitized solar cells. *Electrochimica Acta*, *66*, 151-157. http://dx.doi.org/10.1016/j.electacta.2012.01.088

Wang, H. L., Hao, Q. L., Yang, X. J., Lu, L. D., & Wang, X. (2009). Graphene oxide doped polyaniline for supercapacitors. *Electrochemistry Communications*, *11*(6), 1158-1161. http://dx.doi.org/10.1016/j.elecom.2009.03.036

Xiao, P., Xiao, M., Liu, P., & Gong, K. (2000). Direct synthesis of a polyaniline-intercalated graphite oxide nanocomposite. *Carbon*, *38*(4), 626-628. http://dx.doi.org/10.1016/S0008-6223(00)00005-1

Xiong, S. X., Shi, Y. J., Chu, J., Gong, M., Wu, B. H., & Wang, X. Q. (2014). Preparation of High-performance Covalently Bonded Polyaniline Nanorods/Graphene Supercapacitor Electrode Materials using Interfacial Copolymerization Approach. *Electrochimica Acta*, *127*, 139-145. http://dx.doi.org/10.1016/j.electacta.2014.01.163

Yan, J., Wei, T., Shao, B., Fan, Z. J., Qian, W. Z., Zhang, M. L., & Wei, F. (2010). Preparation of a graphene nanosheet/polyaniline composite with high specific capacitance. *Carbon*, *48*(2), 487-493. http://dx.doi.org/10.1016/j.carbon.2009.09.066

Yang, W. Z., Widenkvist, E., Jansson, U., & Grennberg, H. (2011). Stirring-induced aggregation of graphene in suspension. *New Journal of Chemistry*, *35*(4), 780-783. http://dx.doi.org/10.1039/C0nj00968g

Yang, Y., Diao, M. H., Gao, M. M., Sun, X. F., Liu, X. W., Zhang, G. H., Qi, Z., & Wang, S. G. (2014). Facile Preparation of Graphene/Polyaniline Composite and Its Application for Electrocatalysis Hexavalent Chromium Reduction. *Electrochimica Acta*, *132*, 496-503. http://dx.doi.org/10.1016/j.electacta.2014.03.152

Yi, M., Liang, S. S., Liu, L., Shen, Z. G., Zheng, Y. T., Zhang, X. J., & Ma, S. L. (2014). Investigating the Nature of Graphene-Based Films Prepared by Vacuum Filtration of Graphene Dispersions. *Journal of Nanoscience and Nanotechnology*, *14*(7), 4969-4975. http://dx.doi.org/10.1166/jnn.2014.8648

Yu, P., Li, Y., Zhao, X., Wu, L., & Zhang, Q. (2014). Graphene-Wrapped Polyaniline Nanowire Arrays on Nitrogen-Doped Carbon Fabric as Novel Flexible Hybrid Electrode Materials for High-Performance Supercapacitor. *Langmuir*, *30*(18), 5306-5313. http://dx.doi.org/10.1021/la404765z

Zhang, C., Chen, M., Xu, X., Zhang, L., Zhang, L., Xia, F., Li, X., Liu, Y., & Gao, J. (2014). An Extraordinary Stable Modified Reduced Graphene Oxide Suspension and Its Catalysis. *Science of Advanced Materials*, *6*(4), 760-770. http://dx.doi.org/10.1166/sam.2014.1766

Zhang, J. T., & Zhao, X. S. (2012). Conducting Polymers Directly Coated on Reduced Graphene Oxide Sheets as High-Performance Supercapacitor Electrodes. *Journal of Physical Chemistry C*, *116*(9), 5420-5426. http://dx.doi.org/10.1021/Jp211474e

Zhang, Q. Q., Li, Y., Feng, Y. Y., & Feng, W. (2013). Electropolymerization of graphene oxide/polyaniline composite for high-performance supercapacitor. *Electrochimica Acta*, *90*, 95-100. http://dx.doi.org/10.1016/j.electacta.2012.11.035

Zhu, J., Gu, H., Luo, Z., Haldolaarachige, N., Young, D. P., Wei, S., & Guo, Z. (2012). Carbon Nanostructure-Derived Polyaniline Metacomposites: Electrical, Dielectric, and Giant Magnetoresistive Properties. *Langmuir*, *28*(27), 10246-10255. http://dx.doi.org/10.1021/la302031f